

Nature of particles azimuthal anisotropy at low and high transverse momenta in ultrarelativistic A+A collisions

L V Bravina^{1,2}, G Kh Eyyubova², V L Korotkikh², I P Lokhtin²,
S V Petrushanko², A M Snigirev^{2,3} and E E Zabrodin^{2,1}

¹ Department of Physics, University of Oslo, PB 1048 Blindern, N-0316 Oslo, Norway

² Skobeltsyn Institute of Nuclear Physics, Lomonosov Moscow State University, RU-119991 Moscow, Russia

³ Bogoliubov Laboratory of Theoretical Physics, Joint Institute for Nuclear Research, RU-141980 Dubna, Russia

E-mail: eiyubova@lav01.sinp.msu.ru

Abstract. LHC data on the correlations of the elliptic flow v_2 of particles at low and high transverse momenta p_T from Pb+Pb collisions at center-of-mass energy per nucleon pair $\sqrt{s_{NN}} = 5.02$ TeV are analyzed in the framework of the HYDJET++ model. This model includes soft and hard components which allows to describe the region of both low and high transverse momenta. The origin of v_2 values in different p_T regions is investigated at different centralities. It is shown that the experimentally observed correlations between v_2 at low and high p_T in peripheral lead-lead collisions is due to correlation of particles in jets.

Keywords: Heavy Ion Collisions, Quark-Gluon Plasma, Elliptic Flow, Jet Quenching

1. Introduction

The properties of hot and dense matter produced in heavy ion collisions are thoroughly explored during several decades, especially after the start of heavy-ion programs at the Relativistic Heavy Ion Collider (RHIC) at BNL and the Large Hadron Collider (LHC) at CERN. The focus of the field is to investigate Quark Gluon Plasma (QGP) formation and its characteristics at different conditions. Numerous observables of final event serve to this purpose. Here we study one of the main observables in soft physics sector, namely the azimuthal momentum-space anisotropy of particles, and its manifestation in hard physics regime. The correlations between hard and soft contributions to azimuthal anisotropy of particles have attracted much attention, see [1]–[3].

At relatively low transverse momenta, the azimuthal anisotropy occurs due to the anisotropic expansion of the compressed matter, since particles are emitted preferably in

the direction of the largest pressure gradient [4]. The anisotropy for particles with high transverse momenta is governed by the energy loss of hard partons traversing the hot and dense nuclear medium. Here more jet particles are emitted in the direction of shortest path length [5]. The sizable azimuthal anisotropy observed at RHIC energies was the main evidence for the nearly perfect liquid behavior of the created matter [6, 7, 8, 9]. The parton energy loss in hot and dense medium, so-called jet quenching, can be investigated in experiment with different observables, such as nuclear modification factor of particle, jets suppression. The azimuthal particle asymmetry at high transverse momenta is yet another observable revealing information on jet quenching process. At LHC, the ATLAS [10] and CMS [11] collaborations have performed measurements of the azimuthal anisotropy of charged particles produced in Pb+Pb collisions at $\sqrt{s_{NN}} = 5.02$ TeV up to $p_T = 60$ and 100 GeV/c, respectively.

Anisotropic flow is quantitatively characterized by coefficients in the Fourier expansion of the azimuthal dependence of the invariant yield of particles in a form [12, 13]:

$$E \frac{d^3 N}{dp^3} = \frac{1}{\pi} \frac{d^2 N}{dp_T^2 d\eta} \times \left(1 + \sum_{n=1}^{\infty} 2v_n(p_T, \eta) \cos[n(\varphi - \Psi_{RP})] \right), \quad (1)$$

where φ is the azimuthal angle of particle, η is the pseudorapidity and Ψ_{RP} is the reaction plane angle. The flow coefficients are:

$$v_n = \langle \langle \cos [n(\varphi - \Psi_{RP})] \rangle \rangle, \quad (2)$$

where the averaging is performed over all particles in a single event and over all events. The initial reaction plane angle, which is defined by impact parameter vector, is not known, hence, the direct calculation of v_2 by (2) is not possible. The measurement of collective flow coefficients aims to measure global azimuthal anisotropy, i.e., particle correlations with respect to global event geometry, but the methods of measuring are sensitive to local particle correlations (such as resonance decays, jets, fluctuations and so on). The most advanced experimental techniques, implementing gaps in pseudorapidities between correlating particles, multiparticle cumulant methods and other, suggest suppression of local particle correlations.

The aim of the present paper is to study the correlations between the low- p_T and high- p_T regions of the elliptic flow of charged hadrons in Pb+Pb collisions at $\sqrt{s_{NN}} = 5.02$ TeV at different centralities. These correlations were observed experimentally in [10] and [11]. The origin of the correlations is not understood yet, mainly because of not too many models, such as EPOS [14], QGSJet [15] and HYDJET++ [16] (for recent developments, see also [17] and [18]), which are describing the soft and the hard processes simultaneously. Here we employ the phenomenological model HYDJET++ to explore the behavior of azimuthal particle anisotropies at different transverse momenta and its connection to common global event geometry, and also the feasibility to establish such connection by experimental techniques.

2. HYDJET++ model

We use the HYDJET++ model [16] for nucleus-nucleus collision simulation which combines soft and hard physics as two components of resulting final heavy ion event. The soft physics is based on relativistic hydrodynamics and is represented by the thermal hadronic state generated on the chemical and thermal freeze-out hypersurfaces with preset freeze-out conditions. It includes the longitudinal, radial and elliptic flow effects and the decays of hadronic resonances. The code of it is based on the adapted version of the event generator FASTMC [19, 20]. The particle multiplicity distributions are Poissonians and their mean multiplicities are estimated within the effective thermal volume. The parameters for the soft part need to be tuned to describe experimental data. For instance, the elliptic flow of the produced particles is governed by the spatial and momentum anisotropy of the fireball. The parameter of the spatial anisotropy, $\epsilon_2(b)$, regulates the elliptic profile of the final freeze-out hypersurface at a given impact parameter b . The momentum anisotropy parameter, $\delta(b)$, deals with the modulation of the flow velocity profile. Both parameters are linked via the hydro-inspired parametrization [20]. Parameters responsible for spatial and momentum triangular anisotropy are implemented in the model as well, thus giving rise to triangular and other odd harmonics flow.

The basis for hard physics of nucleus-nucleus collision is elementary QCD parton-parton scatterings as it is realized in PYTHIA [21] with additional simulation of parton energy loss in a dense medium by PYQUEN model [22] with subsequent hadronization. Both collisional loss due to parton rescattering and gluon radiation loss are taken into account when propagating hard parton through a medium. The medium is treated as a boost-invariant longitudinally expanding medium at some temperature with the transverse asymmetric geometry given by impact parameter of a collision (initial elliptic shape is considered). The initial temperature of the medium for central collisions is one of the parameters of the model. The PYQUEN routine is used to generate a single hard nucleon-nucleon (NN) collision. To calculate the mean number of mini-jets produced in A+A collision at a certain impact parameter b one has to (i) determine the number of binary NN collisions in the event and (ii) multiply it to the integral cross section of the hard process. Hardness of the process depends solely on the minimum transverse momentum transfer, p_T^{min} . Therefore, the parameter p_T^{min} is one of the major parameters which regulates the contributions of soft and hard particles to total multiplicity. If the transverse momentum of initial hard scattering does not exceed p_T^{min} , the partons produced in the scattering are excluded from the hard processes. The products of their hadronization are then automatically added to spectrum of hadrons produced in soft processes. Figure 1(a) demonstrates the contribution of the soft and hard components to the formation of elliptic flow in the model. Here the coefficients v_2^{RP} are calculated with respect to the reaction plane. Hydrodynamic nature of elliptic flow of the soft component (shown by red triangles) provides the increasing v_2 with rising p_T . For the hard component, non-zero elliptic flow arises at $p_T > 10$ GeV/ c due to jet

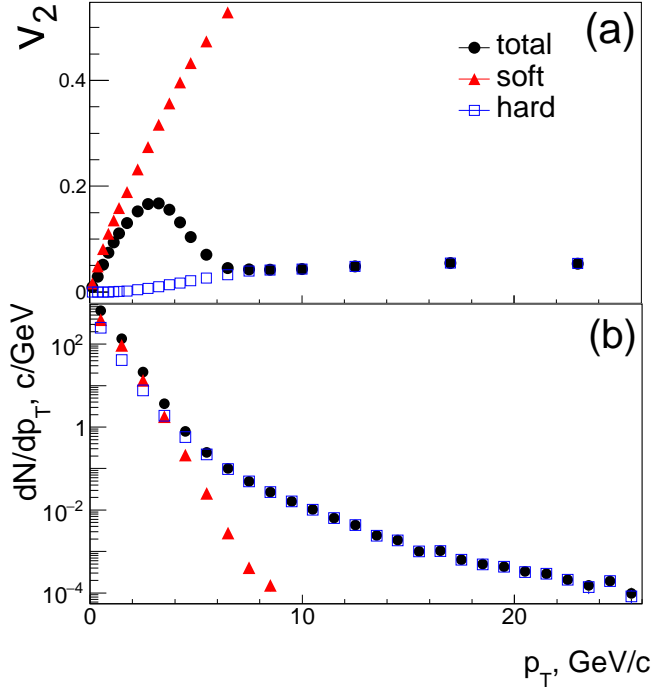


Figure 1. Color online. (a) The elliptic flow as a function of p_T , $v_2^{\text{RP}}(p_T)$, for soft (triangles) and hard (squares) components, and resulting total flow (circles) of charged hadrons with $|\eta| < 2.4$ in 20–30% centrality bin of Pb+Pb collisions calculated within HYDJET++ at $\sqrt{s_{NN}} = 5.02$ TeV. (b) The same as (a) but for the transverse momentum spectra dN/dp_T of charged hadrons for soft and hard components and also the total one.

quenching effect in asymmetric medium. Figure 1(b) shows the spectra dN/dp_T of both components together with total spectrum. At low transverse momenta the multiplicity of soft particles dominates and one can see that the resulting flow in this region is determined mainly by the elliptic flow of soft component, while at high p_T the hard component is dominant and determines total elliptic flow value. In the intermediate p_T region the result is obtained by a simple superposition of two independent contributions.

HYDJET++ model has managed to describe many experimental features and phenomena measured in heavy ion collisions at RHIC and LHC energies. These signals include pseudorapidity and centrality dependence of the multiplicity of charged particles, their transverse momentum spectra, radii of $\pi\pi$ correlations in central Pb+Pb collisions [23], centrality and momentum dependencies of elliptic and higher-order components of the anisotropic flow [24]–[27], flow fluctuations [28], angular dihadron correlations [29], multiplicity correlations of charged particles in forward-backward hemispheres [30], as well as effects of jet quenching [31, 32] and, finally, production of heavy mesons [33]–[35].

3. Calculation of azimuthal anisotropy coefficients

For the correct comparison with CMS data on v_2 of charged particles [11] we apply the scalar product method (SP) and four-particle cumulant method [36]. We do not simulate the detector response, i.e., we use charged particles from the model, but apply the same η -cuts as in experimental data. The two- and four-particle correlations for the second order flow harmonic are defined as

$$\begin{aligned}\langle\langle 2 \rangle\rangle &= \langle\langle e^{i2(\varphi_1 - \varphi_2)} \rangle\rangle, \\ \langle\langle 4 \rangle\rangle &= \langle\langle e^{i2(\varphi_1 + \varphi_2 - \varphi_3 - \varphi_4)} \rangle\rangle,\end{aligned}\tag{3}$$

where double average means averaging over all particle combinations in an event and over all events in a data sample. The estimator of the reference 4-particle cumulant, $c_2\{4\}$, is defined as

$$c_2\{4\} = \langle\langle 4 \rangle\rangle - \langle\langle 2 \rangle\rangle^2\tag{4}$$

For the differential flow calculation one of the particle in (3) is restricted to belong to a certain p_T bin. We denote it by $\langle\langle 2' \rangle\rangle$ and $\langle\langle 4' \rangle\rangle$, respectively. The differential 4-particle cumulant reads

$$d_2\{4\} = \langle\langle 4' \rangle\rangle - 2\langle\langle 2' \rangle\rangle\langle\langle 2 \rangle\rangle.\tag{5}$$

The differential $v_2\{4\}(p_T)$ coefficient is derived as

$$v_2\{4\}(p_T) = -d_2\{4\}(-c_2\{4\})^{-3/4}.\tag{6}$$

The cumulant calculations are based on Q -cumulant method [37], where cumulants are expressed in terms of the corresponding Q_n vectors. The $v_2\{4\}(p_T)$ is calculated in midrapidity region $|\eta| < 2.4$. Methods using many-particle correlations suppose to reflect global collective flow and to suppress local few-particle correlations. CMS measurement of v_2 at high p_T [11] has found similarity of results with 4-, 6-, 8-particle cumulants and also with SP method. The SP method also uses Q_n vectors framework. The Q_2 vector for the second harmonic is defined as

$$Q_2 = \sum_{k=1}^M \omega_k e^{i2\varphi_k},\tag{7}$$

where M is the multiplicity of used particles and ω_k is a weight for a given particle k . Here we use SP method with three subevents, similarly to CMS calculation [11]. Elliptic flow can be obtained as follows

$$v_2\{\text{SP}\} = \langle Q_2 Q_{2A}^* \rangle / \sqrt{\frac{\langle Q_{2A} Q_{2B}^* \rangle \langle Q_{2A} Q_{2C}^* \rangle}{\langle Q_{2B} Q_{2C}^* \rangle}}.\tag{8}$$

The Q_2 vector for sub-events A and B is determined in $-5 < \eta < -3$ and $3 < \eta < 5$ pseudorapidity regions, respectively, and for sub-event C in $|\eta| < 0.75$ region. The vectors Q_{2A} , Q_{2B} and Q_{2C} are calculated with weight ω equal to p_T of particle. The Q_2 vector of particles of interest is calculated in $|\eta| < 1$ pseudorapidity region with the unit weight. If the particle of interest comes with the positive η , then Q_{2A} is calculated using

the negative η region, and vice versa. By its nature, the SP method resembles two-particle correlation methods, but using several sub-events with large η gap suppresses few-particle correlations.

In the model we also calculate elliptic flow v_2^{RP} with respect to reaction plane angle directly with (2). v_2^{RP} is only associated with global event geometry. Figure 2 shows the elliptic flow $v_2\{4\}$, $v_2\{\text{SP}\}$ and v_2^{RP} calculated from the HYDJET++ simulated events with centrality 20–30% and compared to the CMS data [11]. At relatively low transverse momenta, $p_T < 4$ GeV/c, the $v_2\{4\}(p_T)$ and $v_2\{\text{SP}\}$ in HYDJET++ are similar to the generated original elliptic coefficient v_2^{RP} . It is not surprising, because in this momentum region the bulk of the produced particles mainly correlates only with the reaction plane, whereas the non-flow correlations are quite small. The model calculations are also in good agreement with the experimental results. Note, that in the data the difference between $v_2\{\text{SP}\}(p_T)$ and $v_2\{4\}(p_T)$ is more pronounced. The model-generated $v_2\{\text{SP}\}$ is closer to experimentally restored $v_2\{4\}(p_T)$ rather than to $v_2\{\text{SP}\}$. The description of elliptic flow at other centralities can be found in [38]. As was shown in [28], a better quantitative agreement of HYDJET++ results with the data can be reached if both anisotropy parameters, $\epsilon_2(b)$ and $\delta(b)$, are treated as independent ones. In the region of high transverse momenta with $p_T > 10$ GeV/c the model calculations fit to the data fairly well. In the region of intermediate transverse momenta with $4 < p_T < 10$ GeV/c,

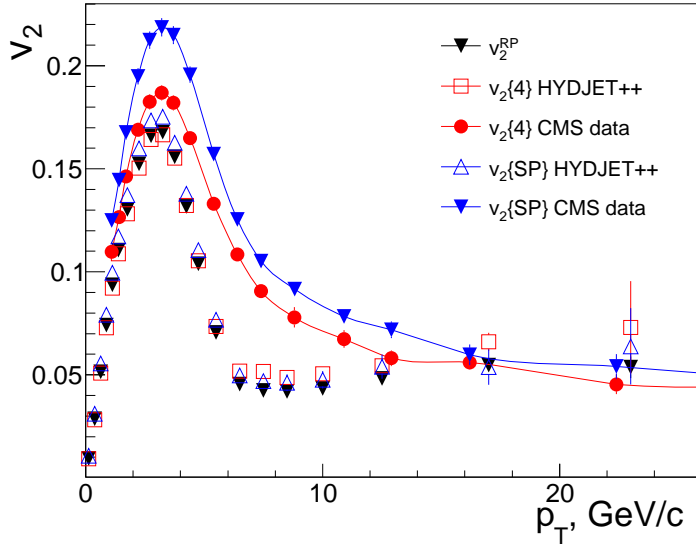


Figure 2. Color online. The comparison of the model elliptic flow with CMS data [11] for $v_2\{4\}(p_T)$ (data: circles; model: open squares) and $v_2\{\text{SP}\}(p_T)$ (data: blue down triangles; model: open triangles) in Pb+Pb collisions at $\sqrt{s_{NN}} = 5.02$ TeV for the centrality 20–30%. The elliptic flow calculated with respect to reaction plane angle in the model, v_2^{RP} , is also shown (black down triangles). Lines are drawn to guide the eye.

where we have transition between soft and hard physics, the model calculations are lower than the experimental data. However, this region is out of scope of our study and, therefore, it does not affect the results of the present work.

4. Elliptic flow correlation at low and high transverse momenta

The lead-lead collisions at $\sqrt{s_{NN}} = 5.02$ TeV were generated within the HYDJET++ for the following centrality intervals: $\sigma/\sigma_{geo} = 5\text{--}10\%$, $10\text{--}15\%$, $15\text{--}20\%$, $20\text{--}30\%$, $30\text{--}40\%$, $40\text{--}50\%$ and $50\text{--}60\%$. The number of generated events for each centrality bin gradually increases from 2×10^6 events for $\sigma/\sigma_{geo} = 5\text{--}10\%$ to 7×10^6 events for $\sigma/\sigma_{geo} = 50\text{--}60\%$. Figure 3 shows the correlations between the elliptic flow of hadrons with transverse momenta $1.0 < p_T < 1.25$ GeV/ c and that of hadrons with quite high transverse momenta, $14 < p_T < 20$ GeV/ c . One can see that the HYDJET++ calculated flows, $v_2\{4\}(p_T)$ shown in figure 3(a) and $v_2\{\text{SP}\}$ displayed in figure 3 (b), demonstrate the same the centrality dependence of the elliptic flow correlations as observed in the experiment. However, elliptic flow values calculated with respect to reaction plane

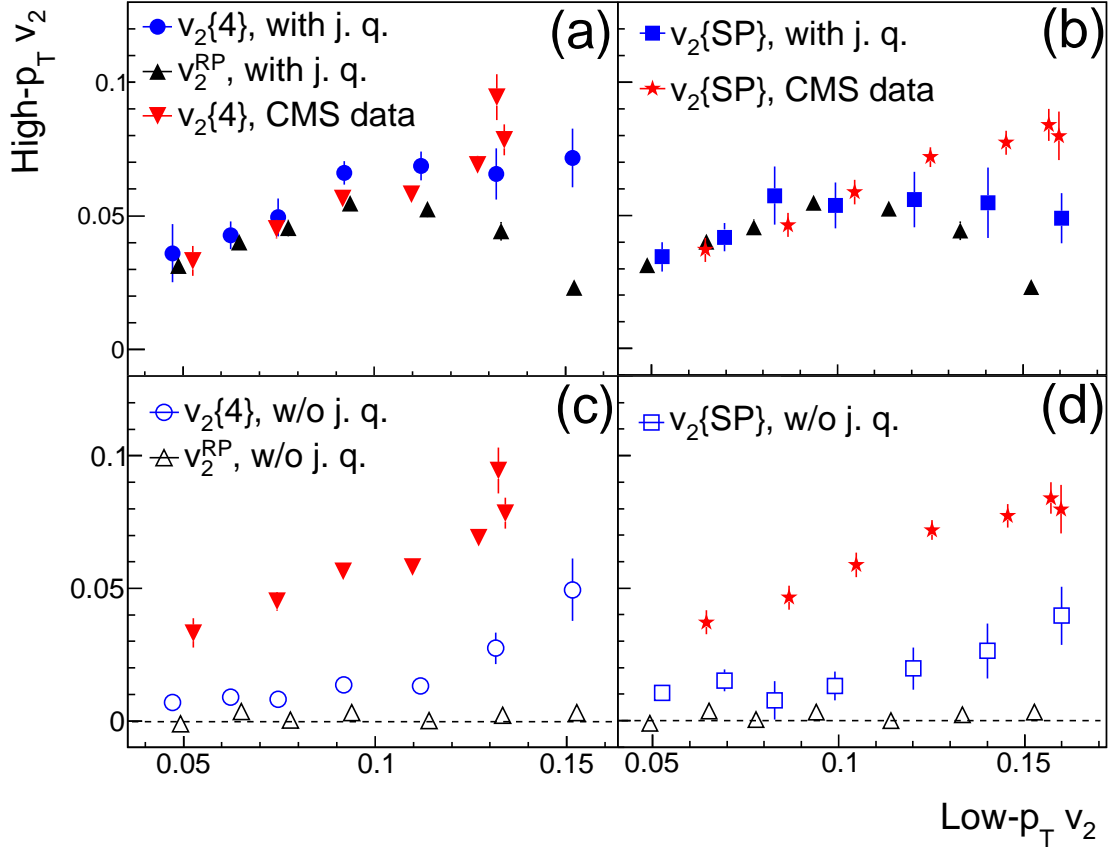


Figure 3. Color online. The centrality dependence of the correlation between elliptic flows of hadrons with low and high transverse momenta in Pb+Pb collisions at $\sqrt{s_{NN}} = 5.02$ TeV. The results are shown for seven centrality bins $5\text{--}10\%$, $10\text{--}15\%$, $15\text{--}20\%$, $20\text{--}30\%$, $30\text{--}40\%$, $40\text{--}50\%$, and $50\text{--}60\%$. Model calculations are presented for v_2^{RP} (black triangles), $v_2\{4\}$ (blue circles) and $v_2\{\text{SP}\}$ (blue squares). CMS data for $v_2\{4\}$ (red down triangles) and $v_2\{\text{SP}\}$ (red stars) are taken from [11]. HYDJET++ calculations are performed also with jet quenching, j. q., (full symbols in (a) and (b)), and without jet quenching, (open symbols in (c) and (d)).

angle, v_2^{RP} , at low and high p_T remain correlated only for semicentral collisions. For centralities larger than 30–40% v_2^{RP} at high p_T begins to die out. Elliptic flow v_2^{RP} at high p_T appears solely due to jet quenching effect. To confirm this one can see the model simulations without jet quenching effect in figure 3(c), where v_2^{RP} at high p_T is consistent with zero. The jet quenching depends not only on path length of parton in a medium, but also on medium density and temperature. For peripheral collisions the asymmetry of path lengths increases but medium density decreases which leads to decreasing of v_2^{RP} at high p_T , see figure 3(a). The coefficients $v_2\{4\}(p_T)$ and $v_2\{\text{SP}\}$ have additional contribution to anisotropy rather than jet quenching effect, as can be seen from figure 3(c), (d). Note that only jets contribute to the spectrum dN/dp_T in this interval of transverse momentum in our approach and, therefore, the anisotropy can be caused by dijet topology. Thus, we can distinguish at least two directions, namely, the jet axis and the reaction plane, relative to which the particles are correlated. The first one becomes more pronounced for peripheral collisions, which can be explained as the follows: in central collisions more jets are produced with random directions, for peripheral collisions the probability of dijet topology increases. The model simulations indicate that in collisions with centrality below 30–40% azimuthal anisotropy occurs due to jet quenching, while in more peripheral collisions, jet particle correlations make a significant contribution to the fourth order cumulant and scalar product methods.

5. Conclusions

The analysis of azimuthal anisotropy coefficients at low and high transverse momenta has been performed for Pb+Pb collisions generated within two-component model HYDJET++ at center-of-mass energy $\sqrt{s_{NN}} = 5.02$ TeV per nucleon pair. Both phenomena, responsible for the origin of azimuthal anisotropy at low and high p_T , namely hydrodynamic expansion of the created matter and jet quenching, are related and sensitive to initial anisotropy of overlap region of nuclei. We have found the correlation of elliptic flow values measured with respect to reaction plane angle, v_2^{RP} , at low and high p_T in central and mid central collisions (up to 40%). For more peripheral collisions the v_2^{RP} at high p_T decreases. Nevertheless, for coefficients measured by cumulant and scalar product methods additional source of azimuthal anisotropy emerges for peripheral collisions, i.e., anisotropy connected to dijet topology. If the centrality of the collisions is 30–40% or less, the four-cumulant and the scalar product methods are sensitive mainly to the azimuthal anisotropy of initial overlapping region. As the collisions become more peripheral, the azimuthal anisotropy begins to be determined primarily by the correlation of particles inside the jets. Combination of these two origins of anisotropy tends to reproduce experimentally observed correlations of the elliptic flow values at different transverse momenta in all centralities.

Acknowledgments

We would like to thank A.I. Demyanov, L.V. Malinina and A.V. Belyaev for fruitful discussions. This work was supported in parts by Russian Foundation for Basic Research (RFBR) under Grants No. 18-02-00155, No. 18-02-40084 and No. 18-02-40085. LVB and EEZ acknowledge support of the Norwegian Research Council (NFR) under grant No. 255253/F50 “CERN Heavy Ion Theory.”

- [1] Armesto N, Salgado C A and Wiedemann U A 2005 *Phys. Rev. C* **72** 064910
- [2] Jia J 2013 *Phys. Rev. C* **87** 061901(R)
- [3] Noronha-Hostler J, Betz B, Noronha J and Gyulassy M 2016 *Phys. Rev. Lett.* **116** 252301
- [4] Ollitrault J Y 1992 *Phys. Rev. D* **46** 229
- [5] Gyulassy M, Vitev I and Wang X -N 2001 *Phys. Rev. Lett.* **86** 2537
- [6] BRAHMS Collaboration (Arsene I *et al*) 2005 *Nucl. Phys. A* **757** 1
- [7] PHOBOS Collaboration (Back B B *et al*) 2005 *Nucl. Phys. A* **757** 28
- [8] STAR Collaboration (Adams J *et al*) 2005 *Nucl. Phys. A* **757** 102
- [9] PHENIX Collaboration (Adcox K *et al*) 2005 *Nucl. Phys. A* **757** 184
- [10] ATLAS Collaboration (Aaboud M *et al*) 2018 *Eur. Phys. J. C* **78** 997
- [11] CMS Collaboration (Sirunyan A M *et al*) 2018 *Phys. Lett. B* **776** 195
- [12] Voloshin S and Zhang Y 1996 *Z. Phys. C* **70** 665
- [13] Poskanzer A M and Voloshin S A 1998 *Phys. Rev. C* **58** 1671
- [14] Werner K, Karpenko I, Bleicher M, Pierog T and Porteboeuf-Houssais S 2012 *Phys. Rev. C* **85** 064907
- [15] Ostapchenko S, 2011 *Phys. Rev. D* **83** 014018
- [16] Lokhtin I P, Malinina L V, Petrushanko S V, Snigirev A M, Arsene I and Tywoniuk K 2009 *Comput. Phys. Commun.* **180** 779
- [17] Chen W, Cao S, Luo T, Pang L-G and Wang X-N 2020 *Phys. Lett. B* **810** 135783
- [18] Pablos D, Singh M, Jeon S and Gale C 2022 arXiv:2202.03414 [nucl-th]
- [19] Amelin N S, Lednicky R, Pocheptsov T A, Lokhtin I P, Malinina L V, Snigirev A M, Karpenko Iu A and Sinyukov Yu M 2006 *Phys. Rev. C* **74** 064901
- [20] Amelin N S, Lednicky R, Lokhtin I P, Malinina L V, Snigirev A M , Karpenko Iu A, Sinyukov Yu M, Arsene I and Bravina L 2008 *Phys. Rev. C* **77** 014903
- [21] Sjostrand T, Mrenna S and Skands P 2006 *J. High Energy Phys.* **0605** 026
- [22] Lokhtin I P and Snigirev A M 2006 *Eur. Phys. J. C* **45** 211
- [23] Lokhtin I P, Belyaev A V, Malinina L V, Petrushanko S V, Rogochaya E P and Snigirev A M 2012 *Eur. Phys. J. C* **72** 2045
- [24] Eyyubova G, Bravina L V, Zabrodin E, Korotkikh V L, Lokhtin I P, Malinina L V, Petrushanko S V and Snigirev A M 2009 *Phys. Rev. C* **80** 064907
- [25] Bravina L, Brusheim Johansson B H, Eyyubova G and Zabrodin E 2013 *Phys. Rev. C* **87** 034901
- [26] Bravina L, Brusheim Johansson B H, Zabrodin E E, Eyyubova G , Korotkikh V L, Lokhtin I P, Malinina L V, Petrushanko S V and Snigirev A M 2014 *Phys. Rev. C* **89** 024909
- [27] Crkovska J *et al* 2017 *Phys. Rev. C* **95** 014910
- [28] Bravina L V, Fotina E S, Korotkikh V L, Lokhtin I P, Malinina L V, Nazarova E N, Petrushanko S V, Snigirev A M and Zabrodin E E 2015 *Eur. Phys. J. C* **75** 588
- [29] Eyyubova G, Korotkikh V L, Lokhtin I P, Petrushanko S V, Snigirev A M, Bravina L V and Zabrodin E E 2015 *Phys. Rev. C* **91** 064907
- [30] Zabrodin E E, Lokhtin I P, Sidorova A A and Chernyshov A S 2020 *J. Exp. Theor. Phys.* **130** 660
- [31] Lokhtin I P, Belyaev A V and Snigirev A M 2011 *Eur. Phys. J. C* **71** 1650
- [32] Lokhtin I P, Alkin A A and Snigirev A M 2015 *Eur. Phys. J. C* **75** 452
- [33] Lokhtin I P, Belyaev A V, Ponimatkin G, Pronina E Yu and Eyyubova G Kh 2016 *J. Phys. G: Nucl. Part. Phys.* **43** 125104

- [34] Lokhtin I P, Belyaev A V, Ponimatkin G, Pronina E Yu and Eyyubova G Kh 2017 *J. Exp. Theor. Phys.* **124** 244
- [35] Lokhtin I P and Sidorova A A 2019 *J. Exp. Theor. Phys.* **128** 586
- [36] Bilandzic A, Snellings R and Voloshin S 2011 *Phys. Rev. C* **83** 044913
- [37] Bilandzic A *et al* 2014 *Phys. Rev. C* **89** 064904
- [38] Bravina L V, Eyyubova G Kh, Korotkikh V L, Lokhtin I P, Petrushanko S V, Snigirev A M and Zabrodin E E 2021 *Phys. Rev. C* **103** 034905